J Fluoresc (2008) 18:305–317
DOI 10.1007/s10895-007-0270-5

ORIGINAL PAPER

pH Induces Thermal Unfolding of UTI: An Implication of Reversible and Irreversible Mechanism Based on the Analysis of Thermal Stability, Thermodynamic, Conformational Characterization

HanDong Fan · Jing Liu · WenDan Ren · ZhongLiang Zheng · YuYing Zhang · Xi Yang · HuaPing Li · XiaoYan Wang · GuoLin Zou

Received: 24 July 2007 / Accepted: 8 October 2007 / Published online: 9 November 2007

Abstract The thermal unfolding of Urinary Trypsin Inhibitor (UTI) was studied by several methods: Circular Dichroism (CD), Fluorescence and UV–Vis spectra. Thermal melting of UTI, dissolved in the neutral and basic buffers, was proved to be irreversible and two domains of UTI unfolded simultaneously, but the melting was reversible and the intermediate was observed when pH is lower than 4.2. The result suggested that heat and changes in pH, which had a more important impact on the stabilization of the domain I and the interaction between two domains, might cause different unfolding transitions. A reasonable explanation was deduced for the mechanism of reversible and irreversible thermal unfolding based on the effect of pH on the protein structure, the analysis of thermal transitions and the result of Electron Microscopy: In neutral and basic buffers, the Reactive Central Loop (RCL) in domain II can interact with or insert into the partial expanding domain I and UTI become self-polymerization, however, no aggregation can be observed in acid buffer since low pH and heat destabilized the structure of the domain I and the native conformation can restructure. The interaction between the special structural element RCL and domain I play an important role in the formation of polymer which was different from other two reasons given by other authors—the cleavage of disulfide and the formation of irregular polymer mainly based on hydrophobic interaction.

Keywords Urinary Trypsin Inhibitor · Thermal unfolding · Thermal stability · Mechanism · pH

H. Fan · J. Liu · W. Ren · Z. Zheng · Y. Zhang · H. Li · G. Zou (✉)
State Key Laboratory of Virology, Life Sciences' College, Wuhan University,
Wuhan 430072, China
e-mail: zouguolin@whu.edu.cn

X. Yang
Chemistry and Molecular Sciences' College, Wuhan University, Wuhan, China

X. Wang
Techpool Bio-pharmaco, GuangZhou, China

Introduction

Structural studies have shown that transitions between different conformations of macromolecules and their complexes are important in biological processes. Some proteins were turned out to be reversible thermal unfolding in acid buffer while irreversible in neutral and basic ones. The typical example was the family of serpin [1–3]. However, it has not been demonstrated why the same protein performed reversible thermal unfolding in acidic buffer while irreversible thermal unfolding usually accompanied with aggregation in neutral and basic one.

Urinary Trypsin Inhibitor (UTI), a kunitz-type protease inhibitor, is effective against a broad range of enzymes including trypsin, chymotrypsin, plasmin, leukocyte elastase and cathepsins B and H. UTI is a single chain protein and its primary structure consists of about 145 amino acid residues and two heavily glycosylated [4]. There are about 21 residues (O-linking region) that precede the N-terminal domain (A22–77, domain I) while the C-terminal domain (A78–133, domain II) is followed by another ten residues.

The fragment (A22–135) has been crystallized and solved [5]. A great deal of attention had been attracted due to the observation that it occurs at elevated levels in several disease states including inflammation and cancer, and under some conditions effectively inhibits tumor invasion and metastasis [6], Presently, UTI is prescribed for the treatment of acute pancreatitis and haemorrhagic shock in Japan and China [7].

We choose UTI as a model protein to investigate the mechanism of reversible thermal unfolding in acidic buffer while irreversible in neutral and basic one. At the same time, as a drug protein, the study of structure and stability mechanism are a basis for improving its stability by other methods and reforming productive techniques in the future.

Materials and methods

Material

UTI was provided by Techpool Bio-pharmaco (GuangZhou, China) and the purity was checked by SDS-PAGE, RP-HPLC. 5,5′-Dithiobis(2-nitrobenzoic acid)(DTNB), Trypsin, *N*-Benzoyl-DL-Arginine-4-nitroanilide-Hydrochloride (BAPNA) and 1-anilino-8-naphthalene sulfonate (ANS),were purchased from Sigma. The buffers were 0.05 M glycine/HCl and 0.2 M NaCl for pH 1.0–3.5, 0.05 M citric acid/Na_2HPO_4 and 0.2 M NaCl for pH 3.5–5.5, 0.2 M phosphate buffer (pH 7.4), 0.05 M glycine/NaOH and 0.2 M NaCl for pH 9.5–12. The solutions were prepared using water filtered through a Mill-Q water system (Millipore, Bedford, MA, USA). The concentration of UTI in all experiments is 60 μg/ml measured by the methods of Coomassie Brilliant Blue G-250.

Size exclusion column of HPLC (SEC-HPLC)

SEC runs were performed on HPLC (Aglient 1100) with a molecular filter column GF250 (Pharmacia). UTI was dissolved in buffers (pH 3.3, 7.4, 9.8) in the presence and absence of 5 M Guanidinium Chloride. Polymer usually disaggregates in the presence of 5 M Guanidinium Chloride, so comparing the retention time in these buffers can detect whether UTI is monomer or polymer.

Steady-state fluorescence spectroscopy

All measurements of steady-state fluorescence spectroscopy were performed on the F-4500 fluorescence spectrophotometer (Shimadzu, Japan) accorded to Roychaudhuri et al. [8]. To determine thermal unfolding profiles, the samples were allowed to equilibrate at each temperature for 10 min before fluorescence readings were taken. A lid was used to prevent evaporation. Thermal unfolding involved progressively increasing the temperature from 293 to 363 K in increments of 5 K. The excitation wavelength was 295 nm for Trp fluorescence measurement but 380 nm for the ANS fluorescence measurement, both excitation and emission bandpasses were 5 nm, and 1 cm light path quartz cuvette was used. The spectra of the buffer were subtracted. To decide whether the thermal unfolding was reversible or not, after each experiment the heated protein sample was cooled to 293 K and the data were measured again.

In order to study the unfolding transition and aggregation in more details through detecting the change of the hydrophobic patch, we performed the same experiments in the presence of a hydrophobic probe ANS. The ANS concentration, 6.25×10^{-6} M and 2.5×10^{-4} M, is about 1/16 and 2.5 times of the maximal association gross with UTI. Both the UTI and ANS were dissolved in the same buffer, pH 3.3 and pH 9.8, respectively.

The anisotropy measurements were performed on a USA PerkinElmer instrument Luminescence spectrometer. Excitation wavelength, quartz cuvette, heating method and excitation and emission bandpasses were the same as the steady-state measurement, but the emission wavelength was 341 nm.

Circular dichroism (CD) measurement

Circular dichroism measurements were performed with a JASCO 8100 spectropolarimeter (Japan) using a quartz cuvette of 0.1 cm optical path. The cuvette containing protein sample was sealed to prevent evaporative loss at high temperature. Temperature regulation was carried out using a JASCO PTC-348WI thermocouple. For CD steady-state measurement, heating method and equilibrating time were the same as the steady-state fluorescence measurement, and the spectra of buffer measured at 298 K were subtracted.

The measurement of UTI inhibitor activity

Trypsin inhibitor activity was measured according to Erlanger et al. [9]. In order to quantify the activity, BAPNA was used as the substrate, and the absorbance value at 410 nm was monitored on a Cary 100 UV–Vis spectrophotometer (Varian, USA). The samples were treated at the same way as the steady-state fluorescence measurement and cooled at the ambient temperature for 24 h. UTI and trypsin were incubated at 310 K for 5 min before BAPNA was added and then incubated for 10 min at the same temperature. Twenty percent acetic acid was used to end the reaction. In our experiments, the substrate is enough and the maximal inhibition activity is about 80%, the rate of inactivity was calculated by the following equation $100\times(A-B)/A$

(A: maximal inhibition activity of the untreated UTI, B: the inhibition activity of the treated UTI).

Measurement of thiol group

UTI, dissolved in the buffer of pH 7.4 and pH 9.8 with 0.5 M Guanidinium Chloride, were incubated in progressively increasing temperature from 293 to 363 K in increments of 5 K. The samples were kept for 10 min at each temperature before 200 μl was taken out, then added into 2 ml 1 mM DTNB which was dissolved in the same buffer composed of 10% ethanol. The 412 nm absorbance values were measured on a Cary 100 UV–Vis spectrophotometer. The references, the heat-untreated DTNB, were subtracted.

In order to detect the effect of high temperature on disulfide of DTNB, 1 mM DTNB dissolved in the buffer of pH 7.4 and pH 9.8 composed of 10% ethanol were heat-treated as the same ways of UTI and the untreated DTNB was subtracted as the reference.

Electron microscopy

Proteins dissolved in deionized water were treated in the same way of thermal denaturation and were cooled at ambient temperature before being applied to carboncoated grids. After 30 s, the drops were blotted, and the grids were stained with 2% phosphotungstic acid for 1 min and then blotted dry. The samples were examined with a Hitachi transmission electron microscope.

Theory

The apparent unfolding fraction measured by fluorescence intensity

The percentage of denatured protein is given by the relation

$$f\alpha = 100(\mathrm{FI}_T - \mathrm{FI_n})/(\mathrm{FI_d} - \mathrm{FI_n}) \quad (1)$$

Where FI_T, is the fluorescence intensity (FI) values at any temperature T, $\mathrm{FI_n}$ for the native protein and $\mathrm{FI_d}$ for the denatured protein. Due to the effects of thermal quenching, $\mathrm{FI_n}$ and $\mathrm{FI_d}$ will both be linear functions of temperature [10]

$$\mathrm{FI_n} = k_1 T + k_2 \quad (2)$$

$$\mathrm{FI_d} = k_3 T + k_4 \quad (3)$$

Where the temperature independent extrapolation parameters k_1 and k_3 are the slope and k_2 and k_4 are the intercept values of FI, and T denotes absolute temperature. Tm is defined as the temperature necessary to produce a thermal unfolding of 50% of all native protein molecules.

The denatured fraction measured by UV–Vis spectra at high pH buffer

The denatured fraction were calculated according to Melo et al. [11]. When the buried tyrosine residues were exposed to the protein surface during the protein unfolding, the side chain phenol groups of tyrosine residues were ionized in the alkaline pH range (pH higher than 9) where the phenolic hydrogen ionization is measurable. Provided the number and the nature of aromatic amino acids of the protein is known, two absorbance measurements, one at 250 nm and the other at 278 nm, are sufficient to obtain the degree of tyrosine ionization in the protein.

The degree of exposure of tyrosine residues at the protein surface was calculated from Eq. 4

$$A = (a + b + c - e - d)/(a - f) \quad (4)$$

Where

a $\mathrm{A278}\varepsilon_{\mathrm{NATyr(OH)A250}}\ \mathrm{N_{Tyr}}$
b $\mathrm{A278}\varepsilon_{\mathrm{NATrpA250}}\mathrm{N_{Trp}}$
c $\mathrm{A278}\varepsilon_{\mathrm{NAPhe250}}\mathrm{N_{Phe}}$
d $\mathrm{A250}\varepsilon_{\mathrm{NATyrA278}}\mathrm{N_{Tyr}}$
e $\mathrm{A250}\varepsilon_{\mathrm{NATrpA278}}\mathrm{N_{Trp}}$
f $\mathrm{A278}\varepsilon_{\mathrm{NATyr(o\text{-})250A}}\mathrm{N_{Tyr}}$

The values of molar absorption coefficient of the different aromatic amino acid derivatives were provided in Table 1.

Analysis of the UV data was based on a two-state model where the equilibrium constant for the unfolded and the folded state of the protein is given by

$$K = (\mathrm{Yf} - Y)/(y - \mathrm{Yu}) \quad (5)$$

Where Yf and Yu, linear functions dependent on temperature, both in pre- and post-transition regions, are the values of a degree of exposure of tyrosine residues at the protein surface characteristic of the folded and unfolded state, respectively, under the temperature where Y is measured. The degree of phenol ionization becomes independent of the protein concentration by the usage of the ratio of absorbance $\mathrm{A_{250}/A_{278}}$ and thus a more accurate value is obtained.

Table 1 Values of molar absorption coefficient of the different aromatic amino acid derivatives

$\mathrm{M^{-1}cm^{-1}}$	$\varepsilon_{\mathrm{NATyr(OH)A}}$	$\varepsilon_{\mathrm{NATyr(o\text{-})}}$	$\varepsilon_{\mathrm{NATrpA}}$	$\varepsilon_{\mathrm{NAPhe}}$
250 nm	390	9,460	2,260	140
278 nm	1,623	1,623	5,640	0

The calculation of thermal stability and thermodynamic parameter

UTI thermal denaturation was determined from the temperature dependence of the equilibrium constant for denaturation K (K=[D]/[N]). A second-order Van't Hoff equation was employed:

$$\mathrm{Ln}K = A + BT^{-1} + CT^{-2} \quad (6)$$

LnK was plotted versus T^{-1} using only results for the apparent unfolding between 0.5 and 0.9. Outside of this range, the ratio of U(D)/N is too large or too small to allow an accurate analysis of results. The parameters A, B and C were determined by non-linear regression. The constants A, B and C are related to thermodynamic parameter. The R value should be larger than 0.98. d(ln$K$)/(d(1/T)=$\Delta H/R$ and d(ΔH)/dT=ΔC. Consequently,

$$\text{At } T = \mathrm{Tm}, \mathrm{Ln}k = 0$$

$$\mathrm{Tm} = 2C \Big/ \left(-B + \left(B^2 - 4AC\right)^{1/2}\right); \Delta\mathrm{Cp} = 2C\mathrm{Tm}^{-2}$$

Results

Monomer

In our experiments, all the samples have the same retention time measured by SEC-HPLC, which indicates UTI is monomer.

Reversible thermal unfolding in acidic buffer but irreversible one in neutral and basic buffer

Probing the reversibility of the process by cooling and reheating, the samples showed that the transition was always irreversible when temperature is higher than the low temperature transformation point when the pH is over 4.2. But for the lower pH the unfolding was reversible even if heated to 363 K, and the initial spectra were regained in heating and cooling cycles.

The effect of pH on Trp microenvironment and the secondary structure of UTI

The effect of pH on tryptophan fluorescence spectra of UTI was investigated over a pH range of 2–11 at the increments of 0.2–0.3 pH. Figure 1a shows that Tryptophan emission has a maximum wavelength at 335 nm, and there is no significant red shift or blue shift when pH is below 9.8, but the emission intensity decreased with increasing or decreasing pH with a midpoint of pH 8.4, an indication that the residue is slightly solvent exposed, as this is the lower or upper limit of the range observed for a buried residues in the apolar protein interior (325–335 nm) [12]. The acid buffers have a more significant effect on Trp microenvironment than the basic ones. An apparent red shift was observed when the pH was higher than 10.5, which implied Trp98 was exposed into the solvent.

The structural changes reflected in the far-UV regions of the CD spectra are usually associated with secondary structure, reorientation of the aromatic amino acids tyrosine and tryptophan, while fluorescence was largely due to emission by exposed or buried tryptophan residue. For detecting the changes of the secondary structure of UTI, the CD was performed.

The effect of pH on the far-UV CD spectra of UTI was also investigated over a pH range of 2–11. The far-UV CD spectrum, a double minimum at 208 and 220 nm, is a typical one of a serpin, where the broad negative minima indicates the presence of both α-helix and β-sheet [13, 14]. Figure 1b shows that there are no significant changes in the native structure of the protein between pH 4.2 and 10.5, as judged by these spectroscopic parameters. While the loss of

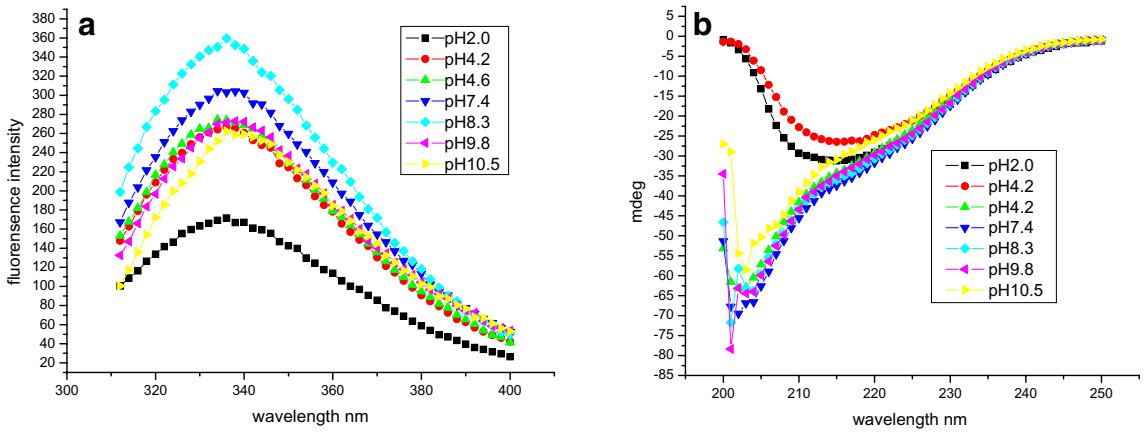

Fig. 1 **a** The fluorescence spectra of UTI which were excited at 295 nm, **b** the CD spectra of UTI. Both were measured at ambient temperature

secondary structure occurred when pH was lower than 4.2, which can be judged from the increase in the CD signal at 200–220 nm [15]. pH deviation from the physiological conditions leads to protonation of the carboxylic groups (decrease of pH)or de-protonation of the amino groups (increase pH) which changed local charges and consequently resulted in repulsions that destabilize the protein. For UTI, the low pH has a stronger effect on the secondary structure.

The effect of heat on Trp microenvironment and the secondary structure

During thermal unfolding, when the temperature changes from 293 K to the low temperature transformation points, the maximal emission wavelength have an 1–2 nm blue shift, while a 5–9 nm red shift can been observed at higher temperature. The Trp emission maximum shifted to 341 nm is a result of a higher but not entire exposition of the Trp to solvent, because the maximal tryptophan emission wavelength would be 348 nm when the residue was entirely solvent exposed [12].

The ratio of Trp fluorescence intensities at 350 and 320 nm ($I_{350}/_{320}$) was used to monitor spectral shifts upon thermal unfolding of UTI [16] as were shown in Fig. 2a and b. The value of I_{350}/I_{320} increased with increasing temperature reveals a red shift which is in agreement with the average microenvironments of Trp98 becoming more hydrophilic. In contrast, the value for $I_{350}/_{320}$ decreased with temperature reveals a blue shift and thus Trp98 was accommodated into a more hydrophobic microenvironment.

Fluorescence anisotropy (R) decays were also measured (Fig. 2c). Fluorescence anisotropy decays provide information on the diffusive motions of a fluorophore during its excited state. Accordingly, the values for decreasing R upon unfolding suggests diminished constrains for the motion of Trp [17], which depolarize intrinsic protein fluorescence [18].

Comparing Fig. 3a,b with c, The increase in ellipticity at 206.5 nm suggests that the fraction of β-turns structures increases with increasing temperature; however, the contributions from a variation in α-helix and β-turn should not be neglected [19]. Mean residue ellipticity at 220 nm changed only to a relatively small extent, which indicated

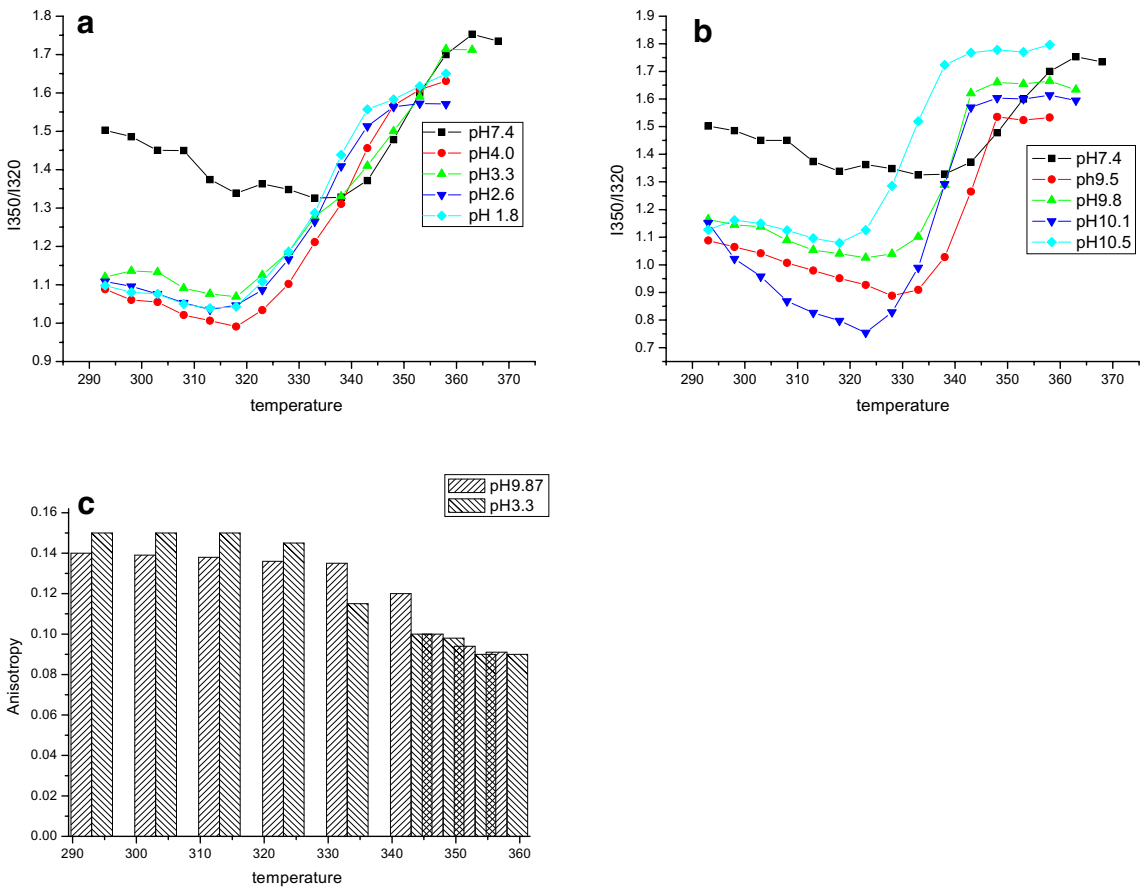

Fig. 2 **a** The ratio I350/I320 versus temperature in acidic buffer; **b** the ratio I350/I320 versus temperature in basic buffer; **c** the anisotropy changes with hoisting temperature

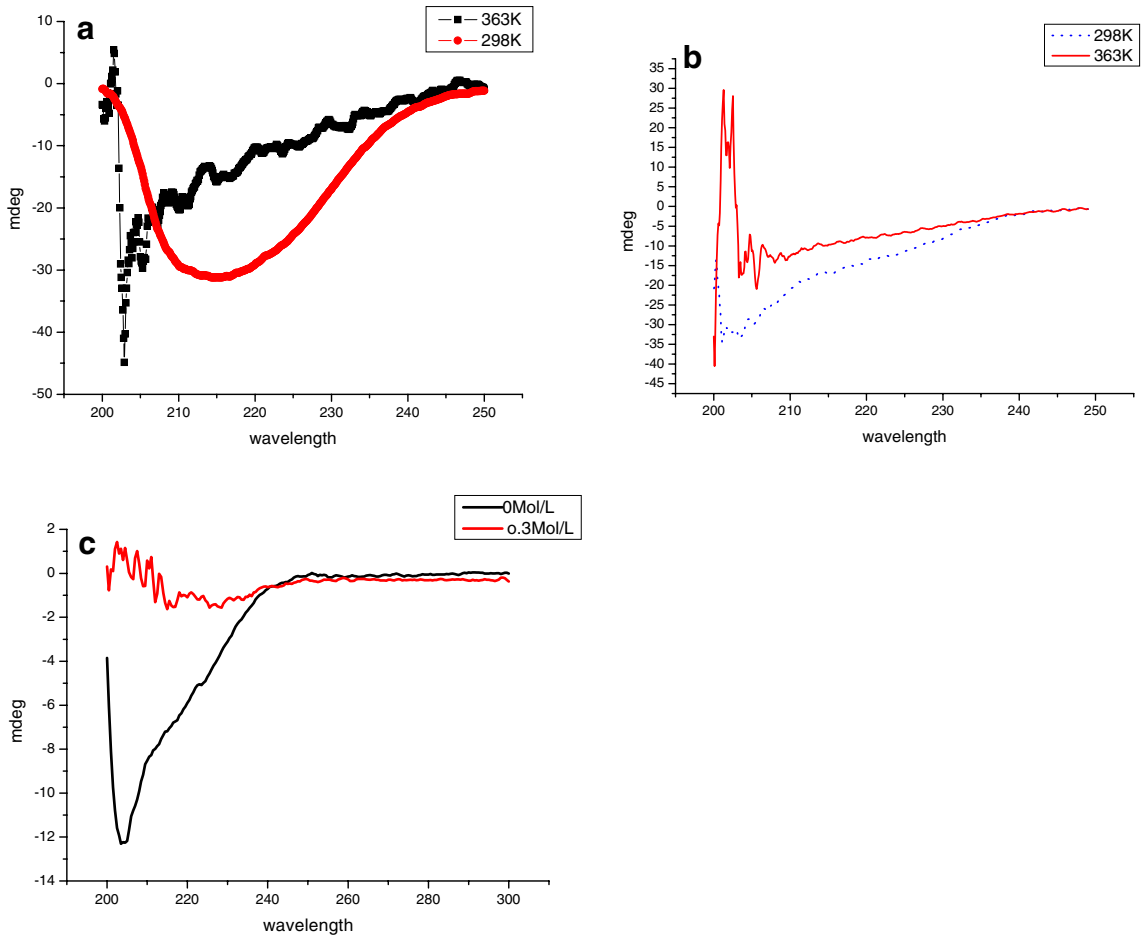

Fig. 3 The CD spectra of UTI at pH 3.3 (**a**) and pH 9.8 (**b**) at 293 K and 363 K; (**c**) the UTI CD spectra in the presence of 0 M and 0.3 M guanidinium chloride at pH 7.4

that the secondary structures of the UTI molecule was only partially dependent on the temperature and existed as a stable molten-global state. This change was different from the spectra of completely denatured UTI dissolved in 0.3 M guanidinium chloride which lost all secondary structures.

Thermal unfolding of domain II

The temperature dependence of fluorescence intensity (FI) 320 nm, FI341 nm and FI365 nm values for UTI can be seen in Fig. 4a. The fluorescence at longer wavelength, e.g.,

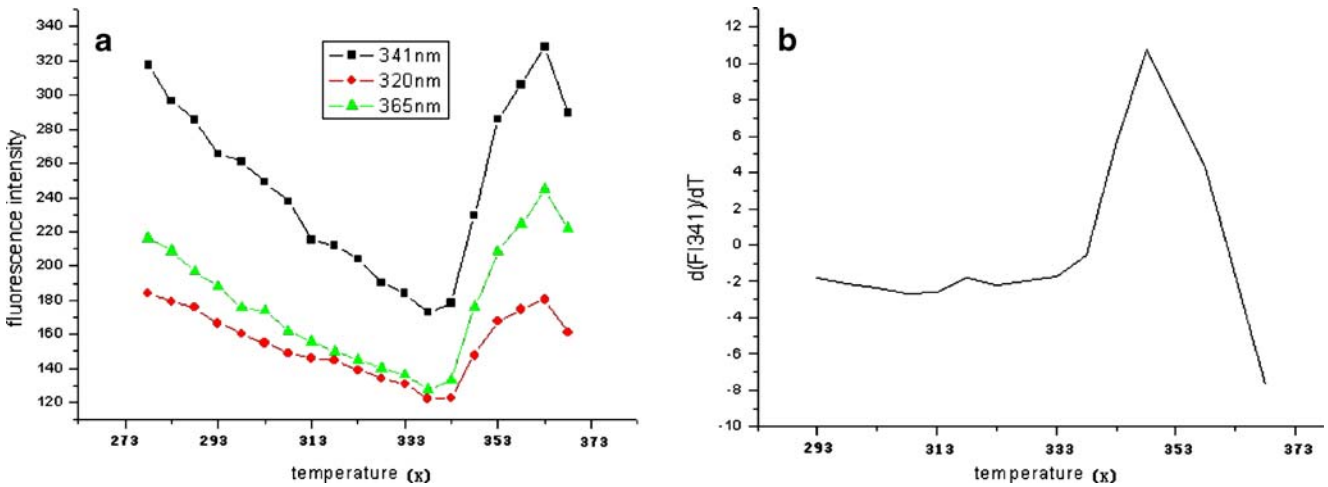

Fig. 4 **a** The plots of fluorescence intensity of 320, 341, 365 nm versus temperature. **b** The plot d(FI341)/d(*T*) versus temperature. For clarity only spectra at pH 7.4 was shown, the others showed the same transitions except occurring at different temperature

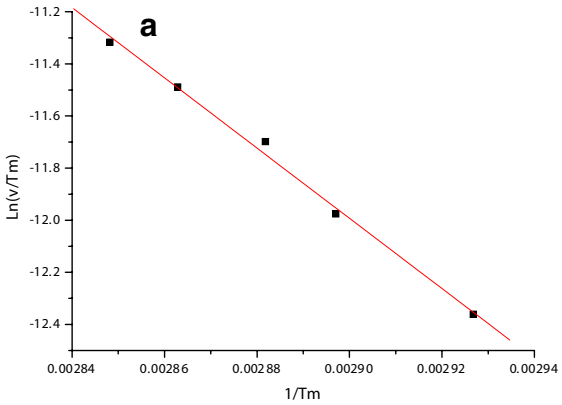

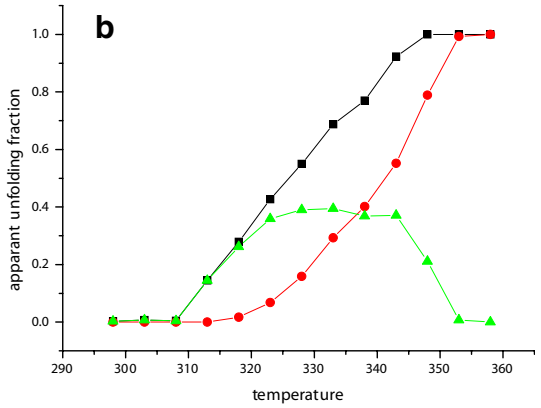

Fig. 5 **a** The linearity Ln(V/Tm^2) versus 1/Tm at the pH 9.8 and the V is 30, 45, 60, 75 and 90 K/h, respectively, measured by CD at 220 nm. **b** *Square*, the unfolding fraction calculated by the CD data at 220 nm, *Diamond*, the unfolding fraction calculated by Trp fluorescence intensity excited at 295 nm, *Triangle*, the differences between them. The experiments were performed at pH 3.3

365 nm, shows "thermal quenching" of the low temperature conformer initially, in the transition region a further increase in intensity and finally a further decrease in intensity reflect "thermal quenching" of the fluorescence of the high temperature conformer [10]. At the low wavelength, e.g., 320 nm, the same conformation transition was observed. The profiles of intensity versus temperature at different pH gave the same transformation except for occurring at the different temperature—the low temperature transformation point (the transition temperature in which the fluorescence intensity changed from decrease to increase in the low temperature region) and the high temperature transformation point (the transition temperature in which the fluorescence intensity changed from increase to decrease in the high temperature region).

The protein denaturation and thermal quenching to the observed FI can be resolved using a first derivative plot of d(FI341)/dT versus T [20]. All the FI341 derivative plot shows a single peak (Fig. 4b), which indicates that the thermal denaturation involved a single transition between native (N) and denatured (D) protein conformation. The data can be fitted well to the Eq. 6. It can be concluded that the thermal unfolding of domain II is a reversible two-state thermal transition in acid buffer while an irreversible two-state thermal transition in neutral and basic buffer.

Thermal unfolding of UTI

The apparent unfolding fraction calculated from UV–Vis spectra can be fitted to the Eq. 6 at the high pH too, at the same time, the CD scanning data at different rate at 220 nm can be well fitted to the equation Ln(V/Tm^2) = Ln(AE/R)− E/(RTm) and shows a good linearity (Fig. 5a). We concluded that there are the same irreversible two-state transition for the whole UTI molecular at the neutral and basic buffer [21]. The almost same Tm value indicated the whole UTI molecular was synchronous unfolding as the domain II. While, at pH 3.3, the apparent unfolding fraction calculated from CD steady-state measurement data at 220 nm can not be fitted to the Eq. 6 and the scanning data had no linearity for Equation Ln(V/Tm^2) = Ln(AE/R)− E/(RTm), which indicated possible intermediate resists. The different value of the apparent unfolding fraction between the result of CD and Trp fluorescence data was calculated as shown in Fig. 5b. The parameters were list in Table 2.

The large positive heat capacity change, five to ten times in the basic buffer as much as in the acid one, is a common feature of both the transfer of nonpolar compounds to water and the temperature-induced denaturation of globular proteins [22]. The decreasing Tm with increasing pH in the basic buffer and decreasing pH in the acid buffer implied pH have an apparent effect on thermodynamic parameters.

Aggregation in neutral and basic buffer in the process of thermal unfolding

For observing the aggregation or the change of molecular volume during the thermal unfolding course, we performed

Table 2 The parameters of the thermal unfolding of UTI

	pH	Tm (K)	ΔCp (K cal deg^{-1} mol^{-1})
F	9.5	336.2	23.0
	9.8	332.8	12.5
	10.1	332.0	11.0
	10.5	329.0	20.7
	4.0	344.3	1.4
	3.3	339.9	0.7
	2.6	334.7	3.7
	2.0	333.6	1.2
U	9.5	336.0	5.8
	9.8	332.0	13.6
	10.1	331.2	5.8
	10.5	328.8	24.4

F Fluorescence spectra, *U* UV–Vis spectra

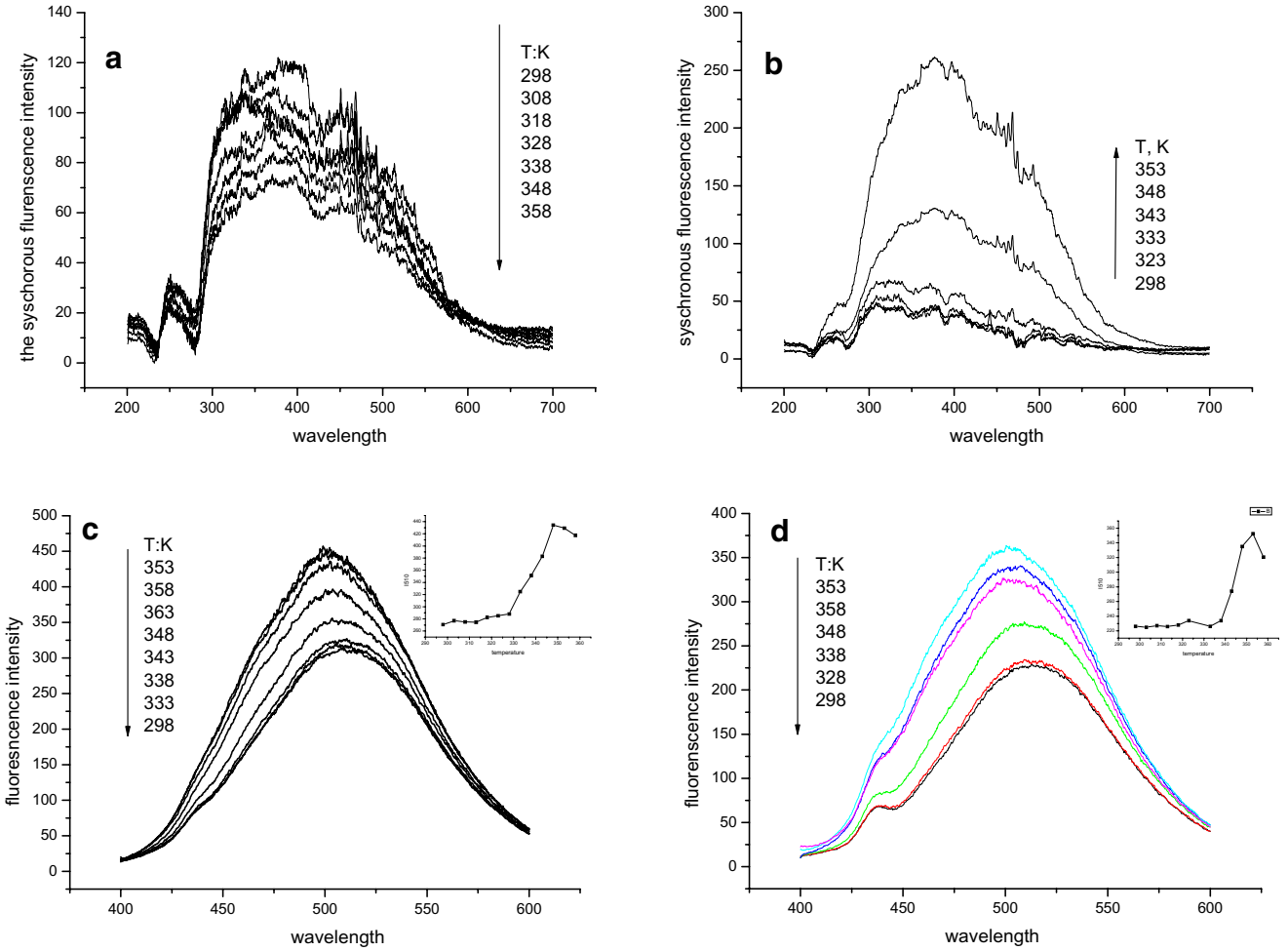

Fig. 6 The aggregation measured based on the light scattering at pH 3.3 (**a**) and pH 9.8 (**b**); The change of hydrophobic patches were detected in the presence of ANS, **c** the concentration of ANS is 2.5×10^{-4} M, pH 9.8; **d** the concentration of ANS is 6.25×10^{-6} M, pH 9.8; **e** the concentration of ANS is 2.5×10^{-4} M, pH 3.3; **f** the concentration of ANS is 6.25×10^{-6} M, pH 3.3; **g** the result of Electron Microscopy at pH 9.8

Rayleigh Scattering (RS). RS was an elastic scattering with the scattering wavelength being equal to the incident wavelength and a good method applied to study biological macromolecule solution for determining molecular weight, the room radius of gyration, shape and size, as well as researching dynamic behavior on the process of reaction [20, 23, 24]. According to the law of RS, when the determination conditions and the concentration of the solution are fixed, the intensity of scattering is proportional to the square of the volume of the particle [25]. It can be seen from the Fig. 6a and b, when the temperature was below the one of low temperature transformation point, the intensity of RS decreased little at both pH 3.3 and pH 9.8. However, when the temperature was higher than the temperature of low temperature transformation point, the intensity of RS at pH 9.8 increased greatly, which showed polymer were formed with hoisting temperature. Contrarily, at pH 3.3, the intensity of RS decreased lightly at all times, which indicated not only there were no aggregation but the UTI molecular volume contracted a little.

The ANS fluorescence spectra implicated the changes of the hydrophobic patch. Only a slight increase in intensity and almost no variation of the average emission wavelength was observed in both pH 3.3 and pH 9.8 when the temperature was lower than the low temperature transformation point, which suggested there was no exposure of hydrophobic patch. While a decrease can be observed when temperature is above high temperature transformation point, which can be explained by the effect of temperature on the association constant between UTI and ANS, and the decrease can be partially overcame by the increasing of ANS concentration. Between the transition region, a significant increase in ANS fluorescence intensity at pH 9.8 was observed accompanied with an obvious blue shift which indicated that ANS in the binding patches has been brought to a more hydrophobic environment that

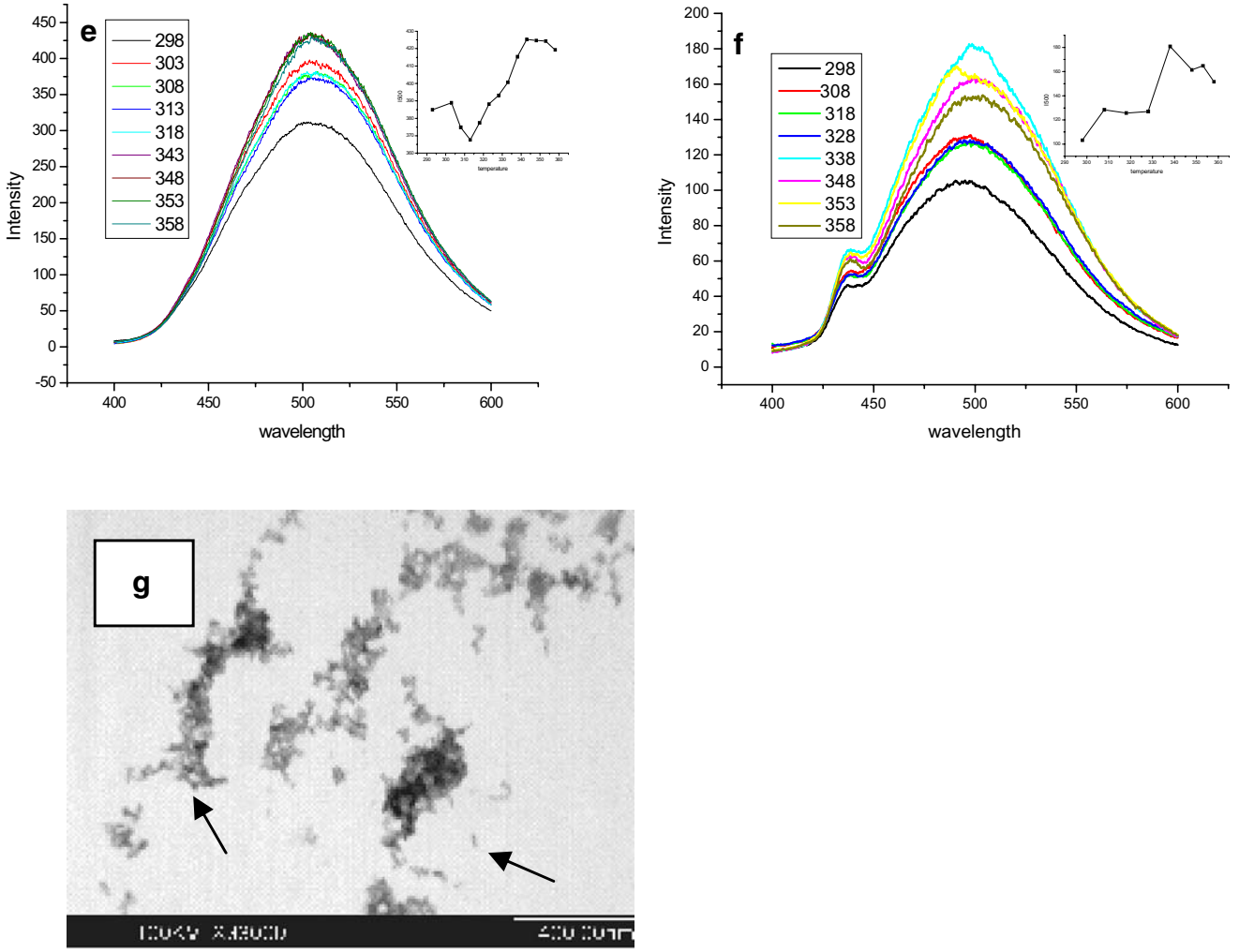

Fig. 6 (continued)

resulted from the aggregation of UTI, while the little red shift in pH 3.3 indicated a more flexible and open conformation [14]. This increase in fluorescence intensity characteristically identifies a relaxed molten state whose clusters of hydrophobic side chains that are not yet fully occluded in the native core structure provides binding sites for ANS and allows ANS more access to the hydrophobic core [26–28]. Comparing Fig. 6c and d with e and f, it can be noticed that there was one transition at pH 9.8 while two transitions at pH 3.3 and a significant acromion can be observed.

The result of Electron microscopy provided direct evidence for the formation of self-polymerization. It can be observed from the Fig. 6g that there are little club-shaped congeries, which is about 20–50 nm in the length and 4–6 nm in the diameter at pH 9.8, while no club-shaped congeries can be observed when pH is 3.3(photo not shown).

Measurement of free thiol

In our experiment, no free thiol was detected during the thermal unfolding of UTI. At the same time, DTNB was used as referent sample to be performed the same thermal treating. There is one disulfide in DTNB, the value of UV–VIS absorption at 412 nm can be measured when the disulfide is cleaved [29]. The result showed no absorption was detected, which implicated disulfide was stable under our experiment condition.

Trypsin inhibition assay

The biochemical activity of a protein is dependent on the maintenance of its native conformation. The structure reformed upon cooling is indeed the native conformation of UTI and not an altered or misfolded species. The thermal inactivation is shown in Fig. 7, when the temperature is

below the low temperature transformation point, the structure of UTI can be reconstructed and the inhibitor activity has no loss, however, when the treating temperature is above high temperature transformation point, activity losses all. The thermostability is determined by the rate of loss of protein activity at high temperature. $T_{1/2}$, the temperature of losing half activity, is 332 K for pH 9.8 and 353 K for pH 7.4 calculated from the data of Fig. 7 which is near to the temperature of Tm in the pH 7.4 and pH 9.8.

Discussion and conclusion

The unfolding of a multi-domain protein could be a complex process because each domain can unfold independently or cooperatively and inter-domain interactions can regulate the overall unfolding process [30–33], as a result, which are typically studied by characterization of the domains in isolation or especial probe through protein expression [34, 35]. This raises questions are as to what extent the properties of the isolated domains are representative of the domains in the native protein and how domain–domain interactions modulate the properties of single domains. The change of Trp98, a native probe in domain II, gives an important indication for the thermal unfolding of domain II. The total unfolding information of the whole molecular may be obtained by the CD spectra measured at 220 nm and the UV–Vis spectra which show the degree of exposure of total tyrosine residues.

As can be seen from Fig. 8, only one Trp in domain II, and the salt links (Arg77 to Glu127 and Glu69 to Lys121) as well as van der Waals interactions between Residues Ala50, Lys70, Leu73 and Gln75 from domain I and Ala80, Ala81, Leu84, Tyr112, Gly117, Asn118, Phe122, Tyr123 and Tyr131 from domain II stabilize the observed domain structure. The total contact area between the two domains is 644 A^2—about 13% of the area of a single domain (3,676 A^2 and 3,609 A^2 for domains I and II respectively) [5]. Variations in pH, leading to protonation of the carboxylic groups or de-protonation of the amino groups changing local charges that result in the abolishment of electrostatic interactions or in repulsions that destabilize the protein, cause conformational changes on a protein and destabilize the hydrophobic core in a gradual manner. The acid buffer had a more apparent effect on the UTI structure inferred from the CD spectra as well as an increased solvent exposure of the Trp. The value of pKa of the β-COOH of Glu is 3.9, so the salts bond can be partially or totally abolished when pH is equal to or lower than 4.2. If we assume that the various domains in a multi-domain protein denature independently, the denaturation of a multi-domain protein can be described by the denaturation of the individual domain and different denaturation routes may exist. The interaction between different domains has a strong impact on unfolding routes. So it is reasonable to assume that: two domains unfolded relatively independently due to stabilizing contributions from salt bridges annulled. When the salt bridges which stabilize the two domains are strong enough, a synchronous unfolding can be observed. We concluded that the interaction intensity between domains have an important effect on the cooperation of the whole molecular unfolding, and a strong interaction possibly gives a synchronous unfolding and immediate state resists in weak interaction.

Interestingly, the Tm is almost the same in the high pH. The protein seemed to cooperatively unfold with the simultaneous melting of both the domain II and the whole molecule, while there are two transitions measured by ANS fluorescence spectra (Fig. 6e and f) and the apparent frac-

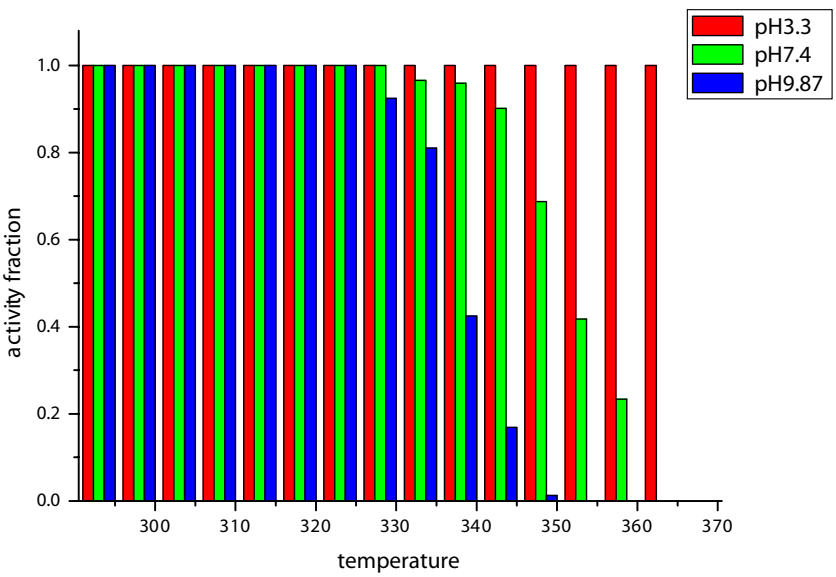

Fig. 7 The plot of the rate of inactivity versus temperature

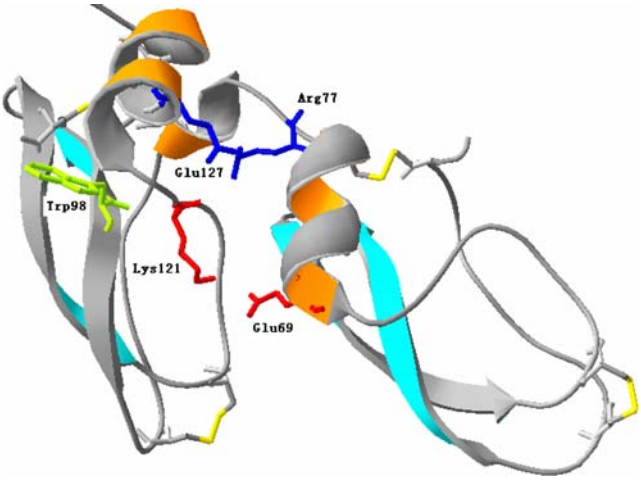

Fig. 8 The sites of six disulfides (*yellow*), Trp98 (*green*) and salt bridges (*red* for Glu69 and Lys121, *blue* for Arg77 and Glu127)

tion measured by CD as 220 nm can not be fitted to the Eq. 6 when pH is 3.3, indicating that there are two different transitions. It also can bee seen from Fig. 6b that the different value between f_{cdI-II} and f_{trpII} is similar to the transition at the low temperature measured by ANS fluorescence spectra, implicating that the two domains unfolded respectively and the domain I maybe have lower thermal stability than domain II in acidic buffer.

The same results for different trypsin inhibitors, heat stable when heated at low or acidic pH while an increased rate of inactivation at elevated temperature as the pH increased from neutral to alkaline, were observed by other investigators [1, 36–40]. Two possible explanations were given for the heat-lability stability, one was the rapid destruction of disulfide bonds and the other was due to aggregation [41, 42]. These samples almost were incubated in boiling water for several hours, but the destruction of disulfide bonds were not detected in our experiment condition.

Certainly, the aggregation was correlative to the inactivation and the irreversible unfolding. However, why aggregation can occur in the neutral and basic buffer but not at the pH lower than 4.2 for the same protein? The question had not been investigated by other authors. The consequent exposure of buried groups to the solvent was responsible for the aggregation of the protein through two different effects. The first one is to provide cross-linking sites at the molecular surface. The second one is a thermodynamic contribution to the onset of protein–protein correlations due to the appearance of an instability region of the protein. The last contribution was found to be responsible for the self-assembly of the protein at very low concentration [43–46]. There are six disulfide bonds in UTI, three of them (Cys 82–Cys 132, Cys 128–Cys 107, Cys 115–Cys 91) (Fig. 8a) were in domain II. Disulfide bonds introduce conformational constraints to main backbone, therefore, stabilize folded proteins in part by restricting the conformational flexibility [47]. Combined with the Trp maximal emission shift to 341 nm and the mean residue ellipticity being changed only to a small extent, we concluded that temperature induced domain II a open but relative rigid molten globular state in either acidic buffer or basic one, but heat and the acid buffer have a more apparent effect on domain I, thereby, we thought the stability of domain I played a pivotal role on the ability of aggregation. Combining the discovery that the RCL of some serpin has the ability to insert into the β-sheet of a second molecule to form well ordered polymers in ambient temperature [46, 48–50], a reasonable hypothesis for the mechanism of reversible or irreversible unfolding of UTI is put forward: When pH is higher than 4.2, the strong interaction between the two domains of UTI relatively stabilizes the structure of domain I and synchronous thermal unfolding occurred. Correspondingly, the partially exposed hydrophobic residues and the partially expanded tertiary structure in domain I provide possible interaction patches for the RCL of domain II, under such circumstances, the head–tail self-polymerization formed which can be directly observed from the photo of electron microscope, and the exposed residues induced by temperature have no ability to be reconstructed to the native conformation. But when pH is lower than 4.2, the loss of second structure and the low thermal stability of domain I make it can not be an appropriate accepter for the RCL of domain II, consequently, self-polymerization could not form, which make it easy to reconstruct the native conformation when reformed upon cooling at ambient temperature.

With previous research findings, there are three main reasons for irreversible unfolding: First, the destruction of disulfide bonds annulled conformational constraints to main backbone; second, part or all of hydrophobic residues were exposed and form a new non-natural conformation molecular or irregular polymer, it is necessary to demonstrate that the exposure of hydrophobic residues is not the sufficient conditions for the formation of polymer, the amount of hydrophobic residues and the relative positions in the first and tertiary structure played an important role, when the hydrophobic residues are comparatively a little or apart from each other too far in tertiary structure, although protein induced by denaturant unfolded completely, it is still difficult to form polymer. Finally, the interaction of some special structural elements is the third reason for the formation of aggregation, obviously, particularity is the most main characteristic of this kind of interaction, for example, the structure of RCL in UTI. We have no reason to think the hydrophobic interaction was the main reason for the formation of regular polymer during the thermal unfolding of UTI, if that were true, the polymer should be easier to form in acid buffer because domain I was more

unstable in acid buffer than neutral and basic one and the hydrophobic residues had greater exposure. Certainly, it is necessary to point out that irregular aggregation can come into being when UTI was incubated for longer time or in higher temperature.

Acknowledgements The authors gratefully acknowledge the National Fund of Nature Science (30370366) and the Research Fund for the Doctoral Program of Higher Education (RFD).

References

1. Baker EC, Mustakas GC (1973) Heat inactivation of trypsin inhibitor, lipoxygenase and urease in soybeans: effect of acid and base additives. J Am Oil Chem Soc 50(5):137–141
2. Flaumenbaum BL, Levitskii AP, Belen'kaia IR (1992) The kinetics of the inactivation of the soybean trypsin inhibitor by heat processing. Ukr Biokhim Zh 64(6):94–98
3. van Den Hout R, Pouw M, Gruppen H, van't Riet K (1998) Inactivation kinetics study of the Kunitz soybean trypsin inhibitor and the Bowman-Birk Inhibitor. J Agric Food Chem 46(1):281–285
4. Hochstrasser K, Schonberger OL, Rossmanith I, Wachter E (1981) Kunitz-type proteinase inhibitors derived by limited proteolysis of the inter-alpha-trypsin inhibitor, V. Attachments of carbohydrates in the human urinary trypsin inhibitor isolated by affinity chromatography. Hoppe Seylers Z Physiol Chem 362(10):1357–1362
5. Xu Y, Carr PD, Guss JM, Ollis DL (1998) The crystal structure of bikunin from the inter-alpha-inhibitor complex: a serine protease inhibitor with two Kunitz domains. J Mol Biol 276(5):955–966
6. Kobayashi H, Kanada Y, Fukuda Y, Yagyu T, Inagaki K, Kondo T, Kurita N, Yamada Y, Sado T, Kitanaka T, Suzuki M, Kanayama N, Terao T (2005) A soybean Kunitz trypsin inhibitor reduces tumor necrosis factor-alpha production in ultraviolet-exposed primary human keratinocytes. Exp Dermatol 14:765–774
7. Shikimi T, Handa, M (1986) Inhibitory effect of human urinary trypsin inhibitor (urinastatin) on lysosomal thiol proteinases. Jpn J Pharmacol 42:571–574
8. Roychaudhuri R, Sarath G, Zeece M, Markwell J (2003) Reversible denaturation of the soybean Kunitz trypsin inhibitor. Arch Biochem Biophys 412:20–26
9. Erlanger BF, Kokowsky N, Cohen W (1961) The preparation and properties of two new chromogenic substrates of trypsin. Arch Biochem Biophys 95:271–278
10. Sommers PB, Kronman MJ (1980) Comparative fluorescence properties of bovine, goat, human and guinea pig alpha lactalbumin. Characterization of the environments of individual tryptophan residues in partially folded conformers. Biophys Chem 11(2): 217–232
11. Melo EP, Aires-Barros MR, Costa SM, Cabral JM (1997) Thermal unfolding of proteins at high pH range studied by UV absorbance. J Biochem Biophys Methods 34(1):5–59
12. Hill JJ, Royer CA (1997) Fluorescence approaches to study of protein-nucleic acid complexation. Methods Enzymol 278:390–416
13. Herve M, Ghelis C (1990) Conformational changes in intact and papain-modified alpha 1-proteinase inhibitor induced by guanidinium chloride. Eur J Biochem 191:653–1658
14. James EL, Bottomley SP (1998) The mechanism of alpha 1-antitrypsin polymerization probed by fluorescence spectroscopy. Arch Biochem Biophys 356(2):296–300
15. Woody RW, Dunker AK (1996) In: Fasman GD (ed) Circular dichroism and the conformational analysis of biomolecules. Plenum, New York
16. Medved LV, Migliorini M, Mikhailenko I, Barrientos LG, Llinas M, Strickland DK (1999) Domain organization of the 39-kDa receptor-associated protein. J Biol Chem 274(2):717–727
17. Lakowicz JR (1999) Principles of fluorescence spectroscopy, 2nd edn. Plenum, New York
18. Steiner RF (1991) Fluorescence anisotropy. In: Lakowicz JR (ed) Topics in fluorescence spectroscopy (vol. 2)
19. Chang CT, Wu CS, Yang JT (1978) Circular dichroic analysis of protein conformation: inclusion of the beta-turns. Anal Biochem 91(1):13–31
20. Burchard W (1991) Combined static and dynamic light scattering approaches to biopolymeric analysis. Biochem Soc Trans 19(2): 478–479
21. Tello-Solis SR, Romero-Garcia B (2001) Thermal denaturation of porcine pepsin: a study by circular dichroism. Int J Biol Macromol 281:29–133
22. Giuseppe Grazianoa FC, Guido B (1998) Prediction of the heat capacity change on thermal denaturation of globular proteins. Thermochim Acta 321:23–31
23. Shinkai S, Yamada S, Kunitake T (1978) Coenzyme models. 10. Rapid oxidation of NADH by a flavin immobilized in cationic polyelectrolytes. Macromolecules 11(1):65–68
24. van den Berg B, Ellis RJ, Dobson CM (1999) Effects of macromolecular crowding on protein folding and aggregation. EMBO J 18:6927–6933
25. Liu S, Luo H, Li N, Liu Z, Zheng W (2001) Resonance Rayleigh scattering study of the interaction of heparin with some basic diphenyl naphthylmethane dyes. Anal Chem 73(16):3907–3914
26. Semisotnov GV, Rodionova NA, Razgulyaev OI, Uversky VN, Gripas AF, Gilmanshin RI (1991) Study of the "molten globule" intermediate state in protein folding by a hydrophobic fluorescent probe. Biopolymers 31(1):119–128
27. Engelhard M, Evans PA (1995) Kinetics of interaction of partially folded proteins with a hydrophobic dye: evidence that molten globule character is maximal in early folding intermediates. Protein Sci 4(8):1553–1562
28. Price NC (2000) Conformational issues in the characterization of proteins. Biotechnol Appl Biochem 31(Pt 1):29–40
29. Krajewska B, Zaborska W (2007) Jack bean urease: the effect of active-site binding inhibitors on the reactivity of enzyme thiol groups. Bioorg Chem 35:355–365
30. Sudharshan E, Rao AG (1999) Involvement of cysteine residues and domain interactions in the reversible unfolding of lipoxygenase-1. J Biol Chem 274:35351–35358
31. Frydman J, Erdjument-Bromage H, Tempst P, Hartl FU (1999) Co-translational domain folding as the structural basis for the rapid de novo folding of firefly luciferase. Nat Struct Biol 6:697–705
32. Sato S, Kuhlman B, Wu WJ, Raleigh DP (1999) Folding of the multidomain ribosomal protein L9: the two domains fold independently with remarkably different rates. Biochemistry 38:5643–5650
33. Llinas M, Marqusee S (1998) Subdomain interactions as a determinant in the folding and stability of T4 lysozyme. Protein Sci 7:96–104
34. He Q, Cederberg H, Rannug U (2002) The influence of sequence divergence between alleles of the human MS205 minisatellite incorporated into the yeast genome on length-mutation rates and lethal recombination events during meiosis. J Mol Biol 319:315–327
35. Santra MK, Banerjee A, Rahaman O, Panda D (2005) Unfolding pathways of human serum albumin: evidence for sequential unfolding and folding of its three domains. Int J Biol Macromol 37:200–204
36. Magdi A, Osman C, Weber W (2002) Thermal inactivation of tepary bean (*Phaseolus acutifolius*), soybean and lima bean protease inhibitors: effect of acidic and basic pH. Food Chem 78:419–423

37. Obara T, Watanabe Y (1971) Heterogenity of soybean trypsin inhibitors. Cereal Chem 48:523–527
38. Wallace GM, Bannatyne WR, Khaleque A (1971) Studies on the processing and properties of soymilk. II. Effect of processing conditions on the trypsin inhibitor activity and the digestibility in vitro of proteins in various soymilk preparations. J Sci Food Agric 22(10):526–531
39. Kwok KC, Qin WH, Tsang JC (1993) Heat inactivation of trypsin inhibitor soymilk at ultra-high temperatures. J Food Sci 58:859–862
40. Despina Galani RKOA (2000) revised equilibrium thermodynamic parameters for thermal denaturation of β-lactoglobulin at pH 2.6. Thermochim Acta 363:137–142
41. Friedman M, Gumbmann MR, Grosjean OK (1984) Nutritional improvement of soy flour. J Nutr 114(12):2241–2246
42. Osman T, Weber CW (1994) Purification and characterization of serine proteinase inhibitor from tepary bean. FASEB J 8:A936
43. San Biagio DBPL, Emanuele A, Palma MU (1996) Self-assembly of physical polymeric gels below the threshold of random crosslink percolation. Biophys J 70:494–499
44. San Biagio VMPL, Emanuele A et al (1999) Interacting processes in protein coagulation. Proteins 37:116–121
45. San Biagio FMPL, Newman J, Palma MU (1986) Sol–sol structural transition of aqueous agarose systems. Biopolymers 25: 2255–2269
46. Zhou A, Faint R, Charlton P, Dafforn TR, Carrell RW, Lomas DA (2001) Polymerization of plasminogen activator inhibitor-1. J Biol Chem 276:9115–9122
47. Bulaj G (2005) Formation of disulfide bonds in proteins and peptides. Biotechnol Adv 23(1):87–92
48. Sivasothy P, Dafforn TR, Gettins PG, Lomas DA (2000) Pathogenic alpha 1-antitrypsin polymers are formed by reactive loop-beta-sheet A linkage. J Biol Chem 275:33663–33668
49. Parmar JS, Lomas DA (2000) Alpha-1-antitrypsin deficiency, the serpinopathies and conformational disease. J R Coll Physicians Lond 34:295–300
50. Carrell RW, Stein PE, Fermi G, Wardell MR (1994) Biological implications of a 3 Å structure of dimeric antithrombin. Structure 2:257–270